ANTIMICROBIAL AGENTS AND CHEMOTHERAPY, May 2005, p. 2035–2043 Vol. 49, No. 5
0066-4804/05/$08.00+0 doi:10.1128/AAC.49.5.2035–2043.2005

Targeting Tn*5* Transposase Identifies Human Immunodeficiency Virus Type 1 Inhibitors

Brandon Ason,[1]† Daniel J. Knauss,[2] Allison M. Balke,[1] George Merkel,[3] Anna Marie Skalka,[3] and William S. Reznikoff[1]*

Department of Biochemistry, University of Wisconsin—Madison, 433 Babcock Drive, Madison, Wisconsin 53706-1544[1]; McArdle Laboratory for Cancer Research, Department of Oncology, University of Wisconsin—Madison, 1400 University Avenue, Madison, Wisconsin 53706-1599[2]; and Fox Chase Cancer Center, Institute for Cancer Research, 333 Cottman Avenue, Philadelphia, Pennsylvania 19111-2497[3]

Received 9 August 2004/Returned for modification 12 October 2004/Accepted 29 December 2004

Human immunodeficiency virus (HIV) type 1 (HIV-1) integrase is an underutilized drug target for the treatment of HIV infection. One limiting factor is the lack of costructural data for use in the rational design or modification of integrase inhibitors. Tn*5* transposase is a structurally well characterized, related protein that may serve as a useful surrogate. However, little data exist on inhibitor cross-reactivity. Here we screened 16,000 compounds using Tn*5* transposase as the target and identified 20 compounds that appear to specifically inhibit complex assembly. Six were found to also inhibit HIV-1 integrase. These compounds likely interact with a highly conserved region presumably within the catalytic core. Most promising, several cinnamoyl derivatives were found to inhibit HIV transduction in cells. The identification of integrase inhibitors from a screen using Tn*5* transposase as the target illustrates the utility of Tn*5* as a surrogate for HIV-1 integration even though the relationship between the two systems is limited to the active site architecture and catalytic mechanism.

Human immunodeficiency virus type 1 (HIV-1) integrase (IN) is a high-valued candidate in the search for new targets to treat human immunodeficiency virus (HIV) infection. IN is responsible for integrating the viral genome into the host, a required step in the viral life cycle (reviewed in references 2, 10, 11, and 19). IN, however, is underutilized for treatment, as only one drug targeting this protein, S-1360, is currently under clinical trials (5), while a second has recently been shown to be effective for rhesus macaques (25). Such candidates would be invaluable to complement existing reverse transcriptase and protease inhibitors used in highly active antiretroviral therapy, the multidrug regime that attenuates HIV.

Many compounds have been identified that inhibit IN in vitro. However, few have been identified that are both specific for IN and effective in cell culture (34). The lack of cocrystal structural information currently available to map critical IN-inhibitor contacts is one limiting factor in the identification of good drug candidates. This information would aid in the rational design or modification of known IN inhibitors to develop more effective therapeutic agents. To date, only partial IN structures have been solved (6, 7, 9, 18, 21, 22, 27, 28, 40, 42) and only two inhibitor classes, diketo and naphthalene derivatives, have been cocrystallized with members of the IN family (21, 27).

Due to these constraints, the Tn*5* transposase (Tnp) may serve as an excellent surrogate model for IN. Tn*5* Tnp is the most extensively structurally characterized member of the Tnp/IN superfamily of proteins (reviewed in references 4 and 13), and although these proteins have low amino acid sequence identity, they share a high degree of structural similarity (4, 7, 15, 18, 36, 40). The catalytic core of this superfamily exhibits an alpha-beta-alpha fold, where two sets of two alpha-helices flank a region of antiparallel beta sheet. Located within this region are three acidic amino acid residues, known as the DDE motif. These residues are responsible for the divalent metal coordination required for catalysis (15, 31). An overlay of Tnp and avian sarcoma virus IN crystal structures reveals that the spatial location of these residues within each protein's active site is surprisingly close, with a root mean square deviation of 0.55 Å (16).

The Tn*5* system provides the only protein-DNA costructural information available for this superfamily, making Tn*5* Tnp an attractive target for inhibitor development. Furthermore, the identification of compounds that cross-react between systems would suggest a similar mechanism of inhibition. Unfortunately, little data exist on inhibitor cross-reactivity between Tn*5* Tnp and HIV-1 IN. Here, we have developed a high-throughput screen to identify compounds that inhibit Tn*5* Tnp-DNA complex assembly, representing the first screen targeting this multimeric protein-DNA complex (16, 32, 36, 37, 41). Since formation of this complex precedes catalysis, inhibitors of this complex would thus inhibit the overall transposition process.

Using this approach, we screened a chemical library for inhibitors of Tn*5* Tnp and identified compounds that inhibit both Tn*5* Tnp and HIV IN in vitro. Several contain substructures found in known integrase inhibitors, and a few inhibit HIV-1 transduction in cells. These results therefore indicate that Tn*5* Tnp can serve as a surrogate for HIV-1 IN. Our results suggest that similar surrogate approaches can be applied for other protein superfamilies, thus allowing one to use

* Corresponding author. Mailing address: Department of Biochemistry, University of Wisconsin—Madison, 433 Babcock Drive, Madison, WI 53706-1544. Phone: (608) 262-3608. Fax: (608) 265-2603. E-mail: reznikoff@biochem.wisc.edu.

† Present address: Hubrecht Laboratory, Uppsalalaan 8, 3584 CT, Utrecht, The Netherlands.

the simplest assays and best available structural data for inhibitor development.

MATERIALS AND METHODS

Compounds. Compound screening was performed at the University of Wisconsin—Madison Comprehensive Cancer Center Small Molecule Screening Facility. This library was originally purchased from ChemBridge. Compound numbers in this report correspond to the following ChemBridge identification numbers: 1, 6160027; 2, 6141194; 3, 6140731; 4, 6158572; 5, 5868253; 6, 6075259; 7, 5980789; 8, 6058083; 9, 6229546; 10, 6176494; 11, 6192779; 12, 5546355; 13, 5535396; 14, 6227564; 15, 5233170; 16, 5232986; 17, 5232985; 18, 6046791; 19, 6044999; 20, 5988232; 10-A, 5789176; 10-B, 6204337; 10-C, 6206397; 10-D, 8065508; 10-E, 6171674; 10-F, 6180772; 10-G, 6215673.

DNA substrates. The oligonucleotides were purchased high-performance liquid chromatography purified from Integrated DNA Technology. Double-stranded DNA (dsDNA) was formed by adding 2 μmoles of each oligonucleotide to 10 mM Tris-HCl, pH 7.9, and 10 mM NaCl. The oligonucleotides were either heated to 96°C for 1 minute followed by a decrease in temperature at 0.1°C/s to 4°C or heated to 90°C in a 2-liter water bath and cooled to 8°C overnight. The transferred strand was 5′ end labeled with either rhodamine green for fluorescence polarization (FP) assays or fluorescein for gel shift assays.

The 19-bp DNA sequences used for FP assays were 5′-C TGT CTC TTA TAC ACA TCT-3′ and its complement. The 40-bp DNA sequences used for the gel shift assays during assay development were 5′-C TGT CTC TTA TAC ACA TCT TGA GTG AGT GAG CAT GCA TGT-3′ and its complement. The 60-bp DNA sequences used for verification of inhibition were 5′-GGC CAC GAC ACG CTC CCG CGC TGT CTC TTA TAC ACA TCT TGA GTG AGT GAG CAT GCA TGT-3′ and its complement.

Tnp and IN purification. The EK54, MA56, and LP372 hyperactive mutant versions of Tnp were used for all assays and are referred to as Tnp throughout this work. Tnp and IN proteins were purified as described previously (3, 38).

Viruses and cell lines. 293T cells were obtained from the American Type Culture Collection. Ghost-R5 (30) cells were obtained from the NIH AIDS Reagent Repository. HIV-1 single-cycle reporter viruses were produced by cotransfection of 293T cells with pNL4-3.Luc.R-E- (12, 26) and HIV-1 Env expression vector pSV7d-JR.FL (17).

FP and gel-shift assays. Reactions were performed as described previously (3), except 800 nM Tnp and 160 nM dsDNA were used for complex formation. For FP analysis, 60-μl reaction mixtures were analyzed using the FP protocol on a Wallac Victor V plate reader, and a 7% native polyacrylamide gel was used in gel shift assays. For compound screening and subsequent analysis, 1 μl of either dimethyl sulfoxide (DMSO) or test compound (final concentration, 80 μM) was added to the synapsis reaction mixtures. Compound screening was carried out using a Beckman Coulter Biomek FX in a 384-well format. Compounds identified as hits were rescreened using gel shift assays under synapsis conditions with a 120 μM compound concentration. Fifty percent inhibitory concentration (IC_{50}) values were obtained by fitting inhibitor titration data (0, 0.01, 0.05, 0.1, 0.5, 2.5, 10, 20, 35, 50, 100, 200, 400, and 800 μM) to an exponential decay.

Inhibition of the restriction enzyme BsmAI was analyzed to determine compound specificity. Reactions were carried out in 2× NEB buffer 3 with 160 nM dsDNA, 10 units of BsmAI (New England Biolabs), and 120 μM lead compound. Reaction mixtures were incubated at 55°C for 1 hour followed by a 20-min 80°C heat inactivation step prior to gel electrophoresis. Samples were loaded onto a 9% native polyacrylamide gel and run at 300 V for 2.5 h. Gels were subsequently imaged and quantitated as described for the synapsis assays.

HIV-1 IN assay. HIV-1 integrase activity was measured as described previously (14), except that 1.0 μl of either DMSO or inhibitor was added to the reaction mixtures. Briefly, HIV-1 IN (1 μM final concentration) was preincubated with various concentrations of inhibitor at 30°C for 30 min. A 21-base pair ^{32}P-labeled substrate (10^6 dpm), representing the U5 end of the viral genome, and $MnCl_2$ (10 mM final concentration) were subsequently added to the reaction mixture. The reaction proceeded for 15 min at 37°C. The reactions were subsequently quenched using EDTA (10 mM final concentration), and the products were separated on a 20% denaturing polyacrylamide gel.

HIV-1 transduction assay and inhibitory screen. Ten thousand Ghost-R5 cells per well were plated in a 384-well plate in 49 μl of medium. Eighteen hours after plating, 1 μl of inhibitory compound, dissolved in DMSO, was added and gently mixed into the solution. Following a 1-h 37°C incubation, HIV-1 virions were added in a final infectious volume of 100 μl. Forty-four to 48 h after infection, 87 μl of medium was removed from each well, and 13 μl/well of Bright-Glo luciferase detection reagent (Promega) was added. After a 2-min incubation, the plates were read on a multiwell plate luminometer.

Cytotoxicity assay. Cytotoxicity assays were performed exactly as the infection assay described above, except medium without virus was added following compound addition and Cell Titer Glo (Promega) viability reagent was added in place of Bright-Glo.

Quantitative real-time PCR of reverse transcripts, detection of transduction in newly infected cells, and effect of compounds on established provirus expression in stably infected cells. Ten thousand Ghost-R5 cells were plated in 96-well dishes, treated with compound in a total volume of 75 μl, and incubated at 37°C for 1 h. Virus was then added in an additional volume of 25 μl. The final infectious volume was 100 μl, the final DMSO concentration was 1%, and the final compound concentration was as indicated. DNA was harvested using the DNeasy kit (QIAGEN) 24 h after infection in the constant presence of inhibitory compounds. Late DNA products of HIV reverse transcription were quantitated using the primers MH531 and MH532 and the probe LTR-P, as described previously (8).

In parallel, cells infected with virus and compound were assayed for luciferase expression by the addition of 100 μl of Bright-Glo reagent, as described above. In this way, the effect of the inhibitory compounds on luciferase expression brought about by successful transduction was measured in the constant presence of the compounds.

To assess the potential effects of the inhibitory compounds on postintegration events such as transcription, translation, and luciferase enzyme stability and activity, Ghost-R5 cells stably infected several weeks earlier with the same virus preparation were incubated with inhibitory compound in 96-well dishes and luciferase activity was monitored 48 h later by the addition of 100 μl of Bright-Glo reagent to each well, as described above.

RESULTS

Identification of Tn*5* Tnp inhibitors. We developed an FP-based, Tnp-DNA complex assembly assay to screen small-molecule libraries for inhibition of Tnp-DNA complex formation. In our assay, we monitored the change in polarization of a fluorescently labeled short DNA fragment containing one Tnp recognition sequence. In general, FP measures the tumbling rate, due to Brownian motion, of a population of fluorescently labeled molecules in solution between the time of fluorophore excitation and emission. Thus, when measuring Tnp-DNA binding interactions, if the percentage of DNA bound by the Tnp increases, the population of more slowly rotating Tnp-bound DNA fragments increases, thereby increasing the FP value.

Comparison of the data obtained using either FP or gel shift assays to monitor Tnp-DNA binding interactions during synapsis reveals that the two assays are in good agreement with one another (Fig. 1). In these experiments, increasing concentrations of an unlabeled DNA were added to the reaction mixture to serve as a competitive inhibitor to Tnp-labeled DNA interactions. These experiments reveal that in each assay the unlabeled DNA reduces the fraction of labeled DNA bound by Tnp within the same concentration range. The observed IC_{50} values are 2.6 ± 0.2 μM and 5.1 ± 0.4 μM for data obtained from the FP and gel shift assays, respectively.

During this initial application, we screened 16,000 pharmacologically active compounds or their derivatives. From this library, 76 compounds were identified as effectors of Tnp-DNA complex assembly. Of these, 20 were identified as inhibitors in several unrelated assays and were therefore considered promiscuous and ignored. Of the remaining compounds, 39 were verified to inhibit complex assembly, as observed by gel shift assays (Fig. 2). To further narrow the number of lead candidates and to focus our search on compounds that were specific to the Tnp/IN superfamily, we tested whether these compounds also inhibited the restriction enzyme BsmAI. This type II restric-

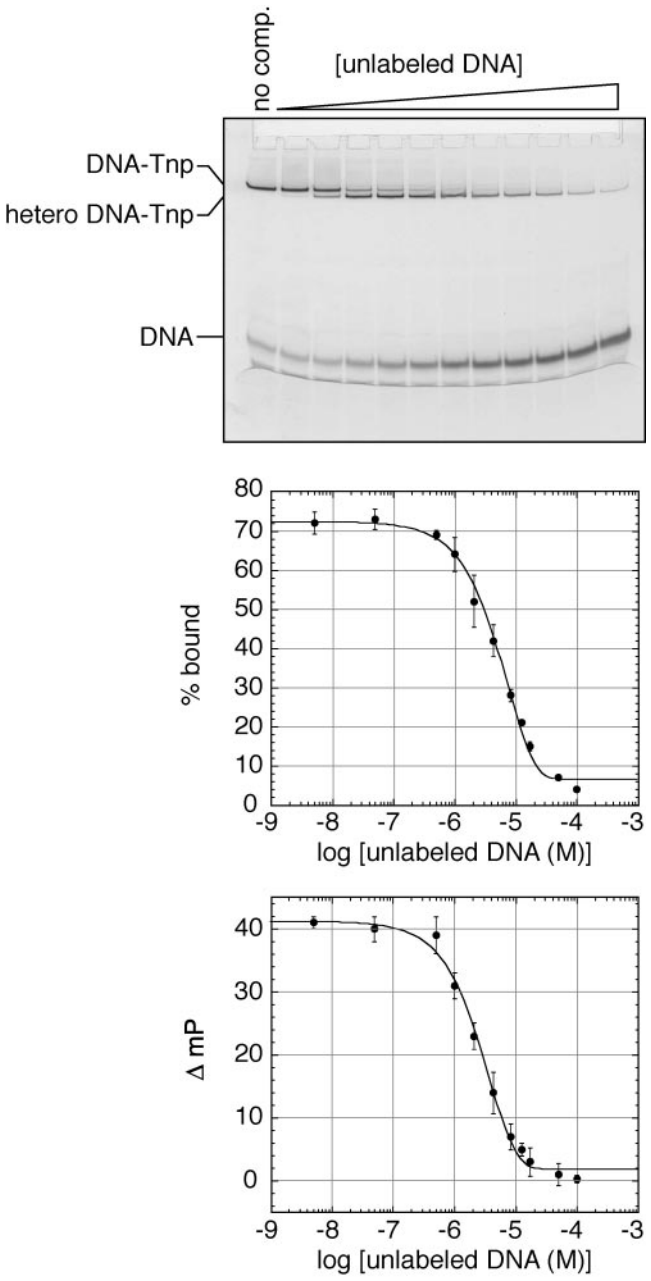

FIG. 1. Comparison of FP and gel shift synapsis assays. FP is a good measurement of the amount of synaptic complexes being formed. Increasing concentrations of unlabeled DNA (0.001, 0.005, 0.01, 0.05, 0.1, 0.5, 1, 2, 5, 8, 10, 20, 50 μM) were used as competitive inhibitors for synaptic complex formation using 160 nM fluorescently labeled DNA and 800 nM Tnp. FP data (bottom) were compared to data obtained using gel shift assays (top). Bands labeled hetero DNA-Tnp represent two dsDNA molecules, one fluorescently labeled and one unlabeled. The lane labeled "no comp." does not contain any unlabeled competitor DNA. IC_{50} values were obtained from fitting these data to an exponential decay and determining the concentration of unlabeled DNA that reduced the amount of fluorescently labeled DNA by one half. IC_{50} values for FP and gel shift assays are 2.6 ± 0.2 μM and 5.1 ± 0.4 μM, respectively, suggesting that FP is a good measurement of the degree of synaptic complex formation. These data were obtained from multiple experiments. Each data point represents the results from at least two, typically three, independent experiments. Error is represented as the standard deviation from the fit of the data to the equation used to calculate the IC_{50}. mP, millipolarization units.

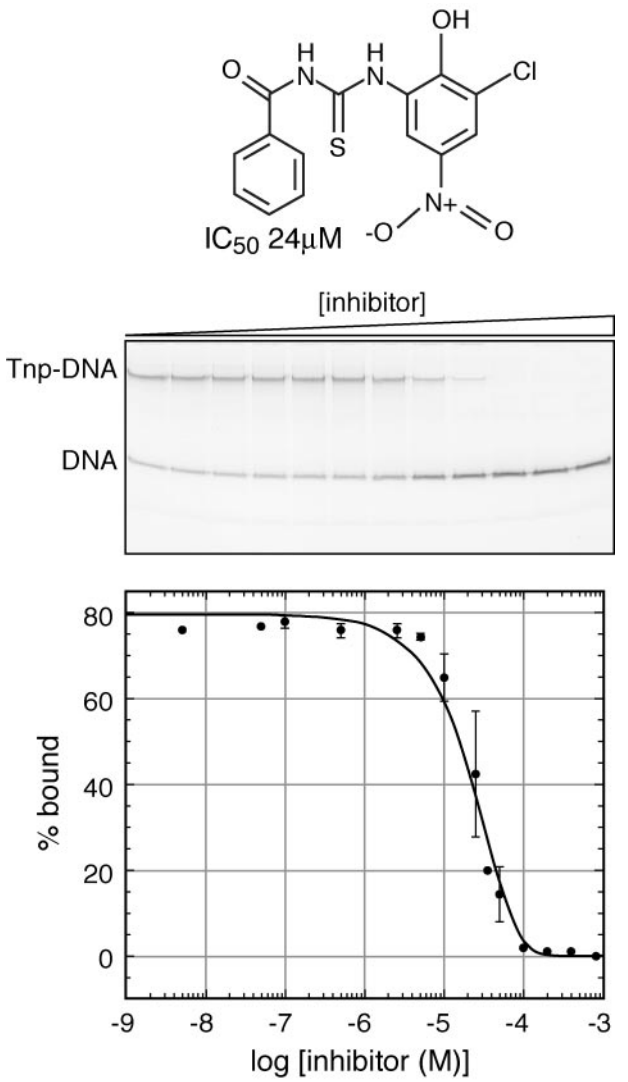

FIG. 2. Verification of Tn*5* Tnp inhibition using gel shift assays. In this example, an aromatic thiourea is shown to be a modest inhibitor of Tnp-DNA complex assembly with an IC_{50} of 24 μM. These values are reported in Fig. 3. The gel shift illustrates compound inhibition of Tnp-DNA complexes in a typical assay and is representative of the data collected for the graph, which was used to calculate an IC_{50} for the inhibitor. The gel shifts observed at low and high inhibitor concentrations are identical to the ones observed for the DMSO only and no-Tnp control reactions, respectively. The data in this graph were obtained from multiple experiments. Each data point represents the results from at least two, typically three, independent experiments. Error is represented as the standard deviation from the fit of the data to the equation used to calculate the IC_{50}.

tion enzyme recognizes a site within the Tnp recognition sequence. Any compound that inhibits BsmAI activity is thus classified a low-specificity Tnp inhibitor. Of these 39 compounds, 20 compounds did not significantly inhibit BsmAI activity.

The 20 compounds that selectively inhibit Tn*5* Tnp are largely aromatic, which is representative of the library as a whole, and exhibit IC_{50} values ranging from 3.5 to 46 μM (Fig. 2 and 3). Within this group, several subsets of compounds appear to be structurally related. One group consists of five

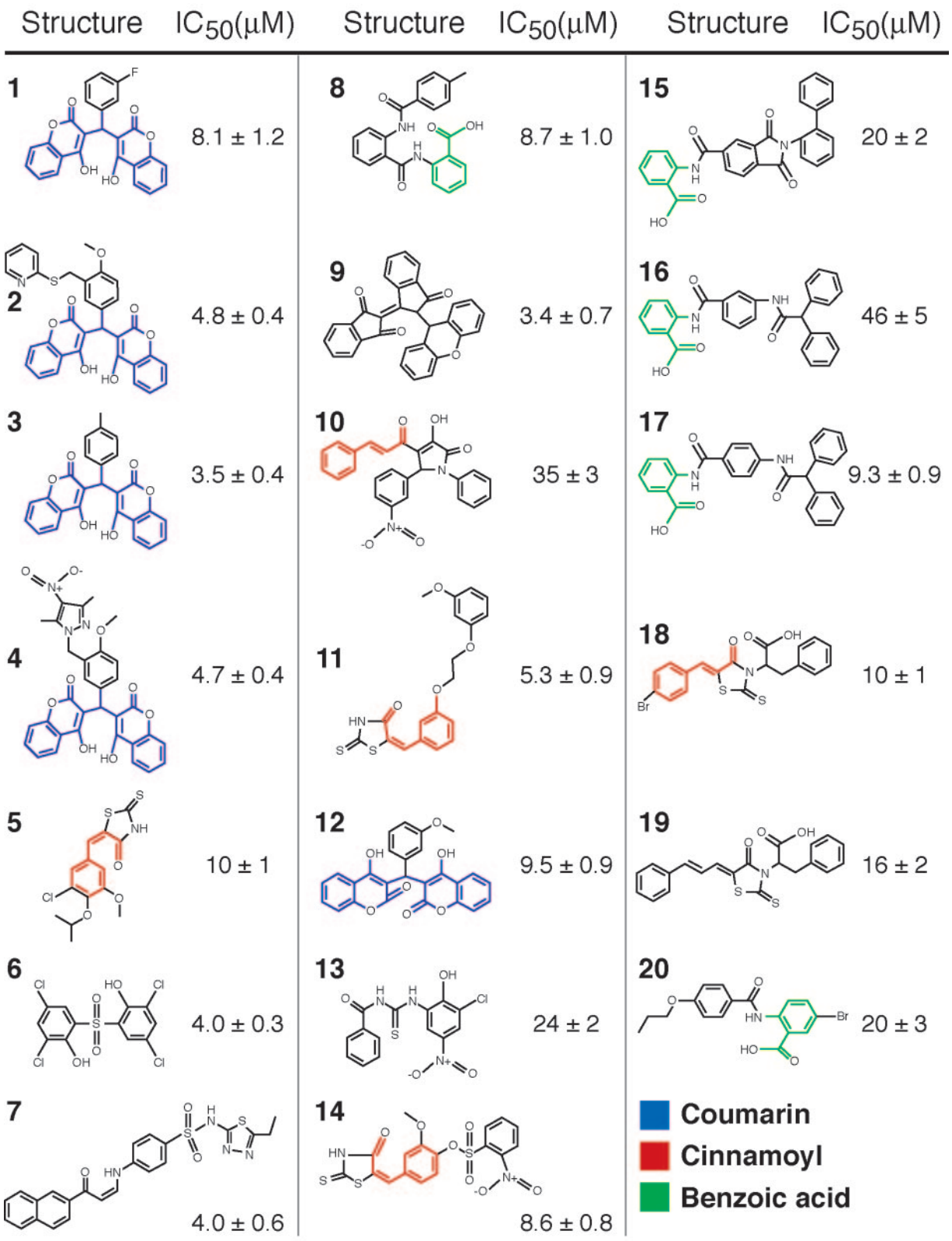

FIG. 3. Twenty compounds are identified that inhibit Tn*5* Tnp-DNA assembly. Several substructures consisting of coumarin, benzoic acid, and cinnamoyl derivatives were identified within this group. The IC_{50} values for these compounds range from 3.4 to 46 μM. IC_{50} values were determined from gel shift assays, similar to those shown in Fig. 2. These data were obtained from multiple experiments. Each value represents the results from at least two, typically three, independent experiments. Error is represented as the standard deviation from the fit of the data to the equation used to calculate the IC_{50}.

coumarin dimers (compounds 1 to 4 and 12). Another consists of benzoic acid derivatives (compounds 8, 15 to 17, and 20). The last group (compounds 5, 10, 11, 14, and 18) contains various conformations of a cinnamoyl moiety. The remaining compounds appear to be unique.

In vitro inhibition of HIV-1 IN. We found that 6 of the 20 compounds that selectively inhibit Tn*5* Tnp also significantly inhibited the activity of HIV-1 IN, as observed by polyacrylamide gel electrophoresis analysis of the reaction products from in vitro integration (Fig. 4 and 5). In an assay with 1 μM HIV IN, the IC_{50} values for these compounds range from 9 to 32 μM. In all cases, IN inhibition is marked by a parallel decrease in the products of both the 3′ strand processing and strand transfer reactions. Inhibition constants were therefore calculated exclusively from the inhibition of 3′ strand processing, as these data were more quantifiable. These inhibitors can be classified into three types of structures, coumarin dimers (compounds 2 and 4), cinnamoyl derivatives (compounds 10, 14, and 18), and a chlorinated bithionol sulfoxide (compound 6).

Inhibition of HIV-1 in cells. These compounds were tested further to determine if they were effective at blocking HIV transduction (a readout for successful integration) in the absence of cytotoxicity. Compound 10, a cinnamoyl derivative, inhibits transduction with a 50% effective dose of 39 μM and an at least twofold-greater 50% lethal dose (Table 1). A search for additional commercially available cinnamoyl-containing compounds resulted in the testing of compounds 10-A through 10-G for their effects on IN in vitro activity, HIV-1 transduction, and cellular toxicity. These studies suggest that the both the ethylene linker within the cinnamoyl moiety and two functional groups located off of the central pyrrole and away from the cinnamoyl play a role in both compound efficacy and toxicity.

Three compounds (10, 10-B, and 10-F) were further tested for their effects on events in the viral life cycle both upstream and downstream of integration. Virus reverse transcripts were quantitated by real-time PCR. Under conditions in which transduction was inhibited by 75% or greater, viral DNA synthesis was either uninhibited or only inhibited to a small extent, suggesting that events up to and including reverse transcription were not affected by the compounds (Fig. 6). To test the effect of the compounds on events after integration, including transcription and translation, and to control for effects on luciferase enzyme stability and activity, cells chronically infected with the same luciferase-encoding HIV-1 virus were assayed in parallel. As shown in Fig. 6, the inhibitory compounds had no effect on luciferase expression in these cells. Finally, the compounds were found to have no significant effect on gross cell viability, as determined using a traditional assay for cellular metabolic activity (Fig. 6). Together, the inhibitory effect of these compounds on Tn*5* Tnp and HIV-1 IN in vitro coupled with their effect in vivo to a point in the viral life cycle post-reverse transcription but upstream of transcription from the provirus suggest that the compounds are inhibiting retroviral integration.

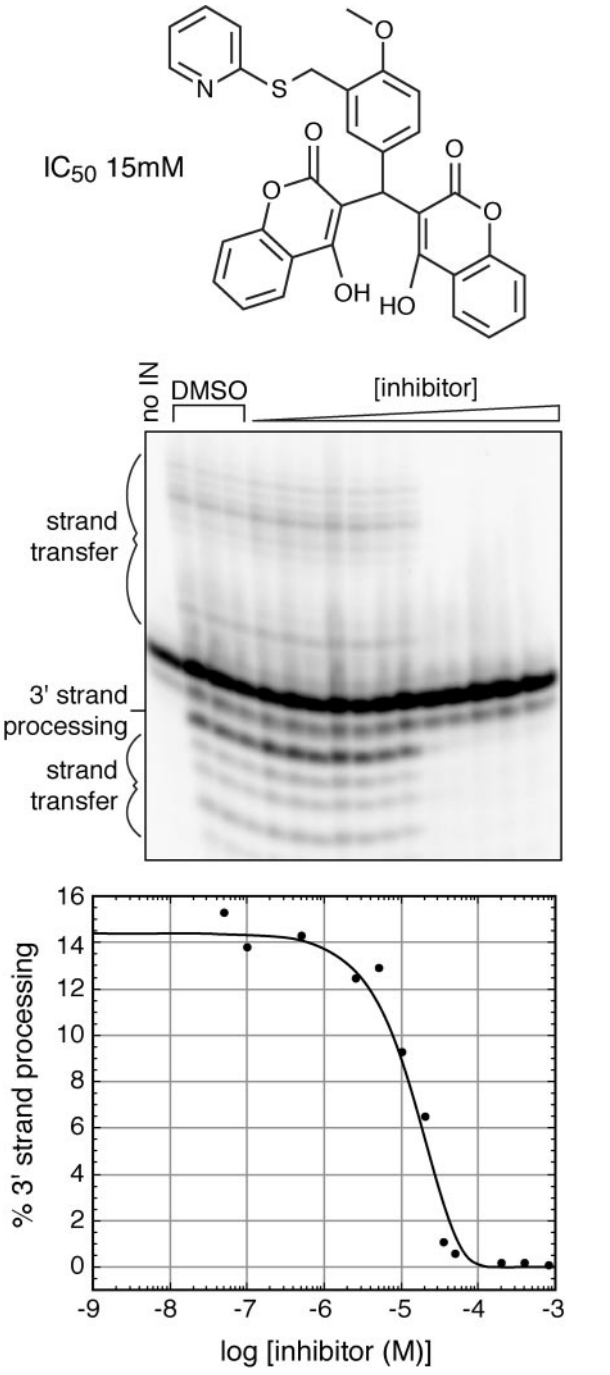

FIG. 4. A large coumarin dimer inhibits IN activity with an IC_{50} of 15 μM. IC_{50}s were determined by measuring the degree of 3′ strand processing that occurs with increasing concentrations of inhibitor (0, 0.05, 0.5, 5, 25, 50, 75, 100, 150, 250, 375, or 500 μM) added to the IN reactions, as described in the Materials and Methods. The degree of 3′ strand processing is measured by the percentage of the signal obtained for the 3′ strand processing product relative to the total signal per lane. These values are reported in Fig. 5.

DISCUSSION

This work provides evidence to support the use of Tn*5* Tnp as a surrogate model for HIV-1 IN inhibitor development. Six compounds were identified that inhibit the activities of both Tn*5* Tnp and HIV-1 IN, yet they do not inhibit the restriction enzyme BsmAI. In addition, these compounds were not identified as hits in any other screen used at the facility, including other FP assays, and it should be noted that for compounds

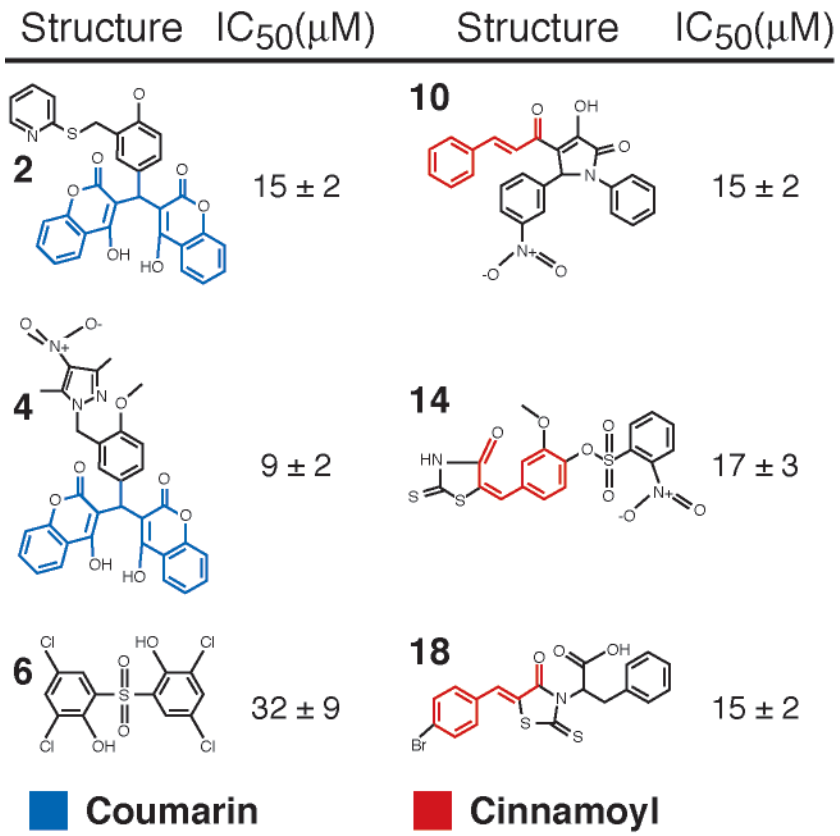

FIG. 5. Six compounds consisting of a biothionol and coumarin and cinnamoyl derivatives inhibit HIV-1 IN activity. The IC_{50} values for these compounds range from 9 to 32 μM. These values are calculated from data measuring the percentage of the 3′ strand processing product formed, as described in the legend to Fig. 4. Assay products are observed using polyacrylamide gel electrophoresis, as described in Materials and Methods. Each value represents the results from at least two, typically three, independent experiments. Error is represented as the standard deviation from the fit of the data to the equation used to calculate the IC_{50}.

tested, inhibition of Tnp synapsis reactions were not affected by the addition of an excess of unlabeled plasmid to chase away any potential inhibition due to nonspecific DNA-compound interactions (data not shown). Thus, the most likely conclusion is that these compounds are not interacting with the DNA but with a region along the protein conserved between Tnp and IN and not BsmAI.

These compounds were originally identified as inhibitors of Tnp complex assembly and are likely inhibiting IN-DNA interactions as well, providing some of the first evidence that both coumarins and cinnamoyl IN inhibitors target this step of the integration mechanism. It has been suggested that IN inhibitors, which target complex assembly, are undesirable because several compounds found to inhibit IN-DNA interactions were shown to be ineffective at inhibiting viral preintegration complexes (20). However, we identified three compounds that inhibit IN in vitro which also inhibit Tnp assembly and HIV-1 infection in cells at a point in the viral life cycle consistent with inhibition of integration (compounds 10, 10-B, and 10-F).

These compounds contain a cinnamoyl moiety attached to a central pyrrole. This cinnamoyl lacks the pharmacophoric aromatic ring hydroxlyations previously described for cinnamoyl inhibitors (1, 8). These previously reported nonhydroxylated cinnamoyls inhibit IN with IC_{50}s in the low micromolar range, which approaches the concentration of Tnp and IN in our in vitro assays, 0.8 and 1.0 μM, respectively. Thus, although these IC_{50} values appear modest, even a very potent inhibitor would not inhibit at a much lower concentration in our assays, since inhibition at stoichiometric levels would occur in the low μM range. This is best illustrated by the fact that cold unlabeled DNA, which serves as a competitive inhibitor, exhibits an IC_{50} of 5.1 μM in our gel shift assay.

Disruption of the cinnamoyl moiety through the removal of the ethylene group (Table 1, compound 10-A) increases cytotoxicity and impedes its efficacy as an IN inhibitor, suggesting that this moiety is important for inhibition. Interestingly, two reactive groups, a ketone and an adjacent enol, form a diketo-like motif within the central pyrrole. This is reminiscent of the diketo moiety found in diketo acids, another extensively described class of IN inhibitors (24). This diketo-like motif is also found in 5ClTEP. In fact, the 5ClTEP IN cocrystal structure revealed that this moiety forms a hydrogen bond with E152 of the IN DDE motif (21). Thus, the activity we observe could stem, in part, from this diketo-like moiety.

However, it is likely that neither the cinnamoyl nor the central pyrrole is the exclusive pharmacophore for these compounds because two additional groups attached to the central

TABLE 1. Relationship between structure and activity for several related compounds reveals two regions that impact cytotoxicity and HIV integration in cells[a]

Structure	HIV-1 transduction ED_{50} (μM)	Cytotoxicity LD_{50} (μM)	HIV-1 IN in vitro IC_{50} (μM)
10 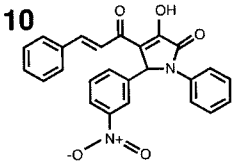	39 ± 10	>100	15 ± 2
10-A 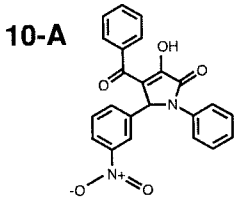	40 ± 8	58 ± 12	165 ± 35
10-B 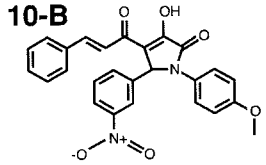	48 ± 8	>100	22 ± 12
10-C 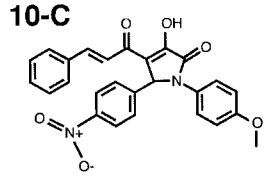	>100	>100	46 ± 12
10-D 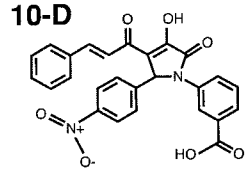	>100	>100	87 ± 9
10-E 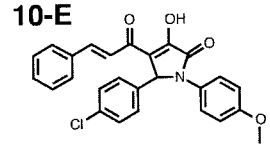	35 ± 6	56 ± 11	12 ± 3
10-F 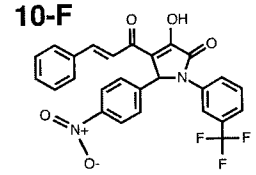	33 ± 17	>100	11 ± 4
10-G 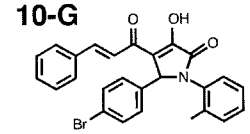	48 ± 18	50 ± 12	11 ± 2

[a] Increasing concentrations (0.01, 0.1, 1, 10, 20, 30, 50, 75, 100 μM) of each compound were used to determine their ability to block HIV-1 integration in vivo and determine their inherent cytotoxicity, as described in Materials and Methods. Reactions were performed in triplicate. Each compound was further analyzed for inhibition of IN activity in vitro, as described in the legend to Fig. 4. Each value represents the results from three independent experiments. Error is represented as the standard deviation from the fit of the data to the equation used to calculate the IC_{50}. ED_{50}, 50% effective dose; LD_{50}, 50% lethal dose.

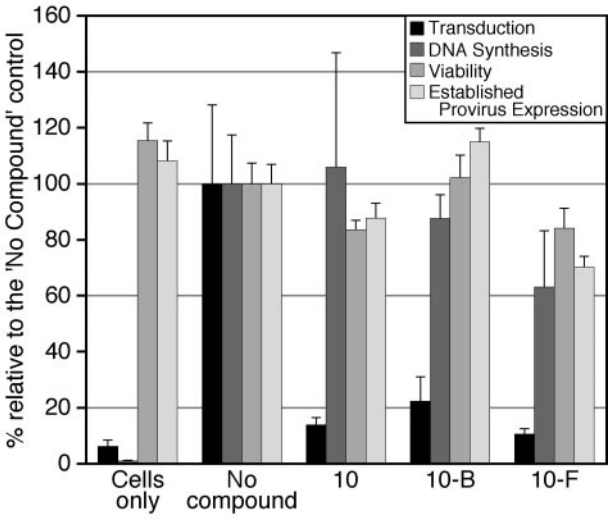

FIG. 6. Inhibitory compounds block HIV-1 transduction in cells at a point in the viral life cycle consistent with inhibition of integration. The inhibitory compounds were simultaneously assayed for their effects on reverse transcription, transduction, gross cell viability, and expression of a stably integrated luciferase-encoding provirus. A quantitative PCR assay was used to monitor effects of the compounds on reverse transcription in acutely infected cells. The compounds were also measured in parallel for their effects on general cell viability and for their effects on expression of luciferase encoded from proviral DNA in chronically infected cells, as described in Materials and Methods. The results demonstrated that compounds 10, 10-B, and 10-F have no significant inhibitory effect on either reverse transcription (or any earlier step in the viral life cycle), cell viability, or luciferase expression. Reactions were performed in triplicate using 75 μM concentrations of each inhibitor.

pyrrole also have an impact on inhibition (Table 1). Furthermore, it is worth noting that compound 10-F partially inhibits BsmAI activity (data not shown), suggesting that although this compound appears to inhibit HIV transduction, it may lack the desired specificity, a phenomenon previously reported for some cinnamoyl derivatives (35). Future studies should therefore involve the identification of related structures that enhance inhibition and specificity without increasing toxicity.

Additionally, we measured compound efficacy against in vivo Tn*5* transposition and determined that none of these compounds had a significant inhibitory effect on transposition in vivo (data not shown). This may stem from poor uptake of these compounds in a bacterial cell culture, and further analysis of inhibition of in vivo transposition should aim at improving the delivery of these compounds into bacteria.

In addition, we found several compounds that appear to represent novel inhibitor classes for this superfamily. Five thiazol derivatives (compounds 5, 11, 14, 18, and 19) were identified as Tnp inhibitors, two of which inhibit both Tn*5* Tnp and HIV-1 IN (compounds 14 and 18). It is noteworthy that the keto group, in combination with the benzene ring and linker, forms a cinnamoyl variant in four of the five thiazol derivatives (compound 5) (Fig. 3). For three of these compounds (compounds 5, 11, and 14) the cinnamoyl is trapped in a configuration not previously reported for IN inhibitors, so it remains unclear whether this moiety is the functioning pharmacophore in these compounds. In addition, several benzoic acids were

identified as Tn*5* Tnp inhibitors (compounds 8, 15, 16, 17, and 20). The similarity between the aromatic diketo acid IN inhibitors and these benzoic acid Tn*5* Tnp inhibitors suggests that this moiety is potentially a pharmacophore in this group.

Several coumarin dimers, one of the most extensively described classes of IN inhibitors, were also identified in this screen. The IC_{50} values we report are, in fact, surprisingly close to those previously reported for similar coumarin derivatives (29, 43). Our results provide the first evidence that coumarins inhibit Tn*5* Tnp, indicating that coumarins are interacting with a conserved region of these proteins. Both this work and previous reports find that potent IN inhibition is limited to coumarins containing large moieties attached to the phenyl linker (43). However, all five coumarins identified in this screen inhibit Tn*5* Tnp at the same approximate concentration, suggesting that the coumarin dimer interacts with a region conserved in both proteins and that the moieties attached to the phenyl linker may interact with a nonconserved region of HIV-1 IN. Modeling coumarin binding using this information could further aid in deciphering the nature of these interactions and in developing more effective coumarin derivatives that specifically inhibit a diverse range of related drug targets.

Our work thus illustrates that Tn*5* is suited as a model for the development of therapeutic agents against HIV-1. Approaches have been reported for both HIV-1 reverse transcription and virus-induced translational frameshifting utilizing components of HIV-1 in alternate systems (23, 33). To identify novel HIV-1 reverse transcription inhibitors, a hybrid Ty1/HIV-1 element was generated, replacing the Ty1 reverse transcription region with that of HIV-1 for use in an inhibitor screen, whereas to study HIV-1-induced translational frameshifting, the HIV-1 −1 frameshift signal was introduced as a transgene in *Saccharomyces cerevisiae*. Both assays serve to aid in identifying and characterizing inhibitors by targeting pieces of HIV-1 in alternate systems, and it is our hope that our approach utilizing a surrogate protein will serve to harness the power of the Tn*5* structural data for the development of improved therapeutics for an alternate step in the viral life cycle.

In conclusion, the success of using Tn*5* transposase as a surrogate for finding HIV-1 inhibitors suggests that similar surrogates can be used for other protein superfamilies. This would facilitate the use of simpler screens and the use of the best available structural data for inhibitor screening and development. This also alerts one to the possibility of undesirable cross activity with other members of the same superfamily of proteins. In this case, such cross-reactivity could occur with the RAG proteins. These proteins are involved in DNA cleavage during immunoglobulin gene formation and have a catalytic mechanism and, presumably, structure similar to both transposase and retroviral integrases (39).

ACKNOWLEDGMENTS

We thank Mindy Steiniger for sharing unpublished data and critically reviewing the manuscript, Laura Vanderploeg for help preparing the figures, and the Small Molecule Screening Facility staff for help with the library screening. The following reagents were obtained through the AIDS Research and Reference Reagent Program, Division of AIDS, NIAID, NIH: Ghost-R5 cells from Vineet N. Kewal-Ramani and Dan Littman and pNL4-3.Luc.R-E- plasmid from Nathaniel Landau. The pSV7D-JR.FL plasmid was a generous gift from T. Dragic.

This work was supported by NIH grants GM 50692, AI 40385, and CA 71515 and by an appropriation from the Commonwealth of Pennsylvania.

REFERENCES

1. **Artico, M., R. Di Santo, R. Costi, E. Novellino, G. Greco, S. Massa, E. Tramontano, M. E. Marongiu, A. De Montis, and P. La Colla.** 1998. Geometrically and conformationally restrained cinnamoyl compounds as inhibitors of HIV-1 integrase: synthesis, biological evaluation, and molecular modeling. J. Med. Chem. **41:**3948–3960.
2. **Asante-Appiah, E., and A. M. Skalka.** 1997. Molecular mechanisms in retrovirus DNA integration. Antiviral Res. **36:**139–156.
3. **Ason, B., and W. S. Reznikoff.** 2004. DNA sequence bias during Tn5 transposition. J. Mol. Biol. **335:**1213–1225.
4. **Berg, D. E., and M. M. Howe (ed.).** 1989. Mobile DNA, 1st ed. American Society for Microbiology, Washington, D.C.
5. **Billich, A.** 2003. S-1360 Shionogi-GlaxoSmithKline. Curr. Opin. Investig. Drugs **4:**206–209.
6. **Bujacz, G., M. Jaskolski, J. Alexandratos, A. Wlodawer, G. Merkel, R. A. Katz, and A. M. Skalka.** 1996. The catalytic domain of avian sarcoma virus integrase: conformation of the active-site residues in the presence of divalent cations. Structure **4:**89–96.
7. **Bujacz, G., M. Jaskolski, J. Alexandratos, A. Wlodawer, G. Merkel, R. A. Katz, and A. M. Skalka.** 1995. High-resolution structure of the catalytic domain of avian sarcoma virus integrase. J. Mol. Biol. **253:**333–346.
8. **Burke, T. R., Jr., M. R. Fesen, A. Mazumder, J. Wang, A. M. Carothers, D. Grunberger, J. Driscoll, K. Kohn, and Y. Pommier.** 1995. Hydroxylated aromatic inhibitors of HIV-1 integrase. J. Med. Chem. **38:**4171–4178.
9. **Chen, J. C., J. Krucinski, L. J. Miercke, J. S. Finer-Moore, A. H. Tang, A. D. Leavitt, and R. M. Stroud.** 2000. Crystal structure of the HIV-1 integrase catalytic core and C-terminal domains: a model for viral DNA binding. Proc. Natl. Acad. Sci. USA **97:**8233–8238.
10. **Chiu, T. K., and D. R. Davies.** 2004. Structure and function of HIV-1 integrase. Curr. Top. Med. Chem. **4:**965–977.
11. **Coffin, J. M., S. H. Hughes, and H. E. Varmus.** 1997. The retroviruses. Cold Spring Harbor Laboratory Press, Cold Spring Harbor, N.Y.
12. **Connor, R. I., B. K. Chen, S. Choe, and N. R. Landau.** 1995. Vpr is required for efficient replication of human immunodeficiency virus type-1 in mononuclear phagocytes. Virology **206:**935–944.
13. **Craig, N. L., R. C., M. Gellert, and A. M. Lambowitz (ed.).** 2002. Mobile DNA II. ASM Press, Washington, D.C.
14. **Daniel, R., C. B. Myers, J. Kulkosky, K. Taganov, J. G. Greger, G. Merkel, I. T. Weber, R. W. Harrison, and A. M. Skalka.** 2004. Characterization of a naphthalene derivative inhibitor of retroviral integrases. AIDS Res. Hum. Retrovir. **20:**135–144.
15. **Davies, D. R., L. M. Braam, W. S. Reznikoff, and I. Rayment.** 1999. The three-dimensional structure of a Tn5 transposase-related protein determined to 2.9-A resolution. J. Biol. Chem. **274:**11904–11913.
16. **Davies, D. R., I. Y. Goryshin, W. S. Reznikoff, and I. Rayment.** 2000. Three-dimensional structure of the Tn5 synaptic complex transposition intermediate. Science **289:**77–85.
17. **Deng, H., R. Liu, W. Ellmeier, S. Choe, D. Unutmaz, M. Burkhart, P. Di Marzio, S. Marmon, R. E. Sutton, C. M. Hill, C. B. Davis, S. C. Peiper, T. J. Schall, D. R. Littman, and N. R. Landau.** 1996. Identification of a major co-receptor for primary isolates of HIV-1. Nature **381:**661–666.
18. **Dyda, F., A. B. Hickman, T. M. Jenkins, A. Engelman, R. Craigie, and D. R. Davies.** 1994. Crystal structure of the catalytic domain of HIV-1 integrase: similarity to other polynucleotidyl transferases. Science **266:**1981–1986.
19. **Esposito, D., and R. Craigie.** 1999. HIV integrase structure and function. Adv. Virus Res. **52:**319–333.
20. **Farnet, C. M., B. Wang, J. R. Lipford, and F. D. Bushman.** 1996. Differential inhibition of HIV-1 preintegration complexes and purified integrase protein by small molecules. Proc. Natl. Acad. Sci. USA **93:**9742–9747.
21. **Goldgur, Y., R. Craigie, G. H. Cohen, T. Fujiwara, T. Yoshinaga, T. Fujishita, H. Sugimoto, T. Endo, H. Murai, and D. R. Davies.** 1999. Structure of the HIV-1 integrase catalytic domain complexed with an inhibitor: a platform for antiviral drug design. Proc. Natl. Acad. Sci. USA **96:**13040–13043.
22. **Goldgur, Y., F. Dyda, A. B. Hickman, T. M. Jenkins, R. Craigie, and D. R. Davies.** 1998. Three new structures of the core domain of HIV-1 integrase: an active site that binds magnesium. Proc. Natl. Acad. Sci. USA **95:**9150–9154.
23. **Harger, J. W., and J. D. Dinman.** 2003. An in vivo dual-luciferase assay system for studying translational recoding in the yeast Saccharomyces cerevisiae. RNA **9:**1019–1024.
24. **Hazuda, D. J., P. Felock, M. Witmer, A. Wolfe, K. Stillmock, J. A. Grobler, A. Espeseth, L. Gabryelski, W. Schleif, C. Blau, and M. D. Miller.** 2000. Inhibitors of strand transfer that prevent integration and inhibit HIV-1 replication in cells. Science **287:**646–650.
25. **Hazuda, D. J., S. D. Young, J. P. Guare, N. J. Anthony, R. P. Gomez, J. S. Wai, J. P. Vacca, L. Handt, S. L. Motzel, H. J. Klein, G. Dornadula, R. M. Danovich, M. V. Witmer, K. A. Wilson, L. Tussey, W. A. Schleif, L. S.**

Gabryelski, L. Jin, M. D. Miller, D. R. Casimiro, E. A. Emini, and J. W. Shiver. 2004. Integrase inhibitors and cellular immunity suppress retroviral replication in rhesus macaques. Science **305:**528–532. (First published 8 July 2004; doi:10.1126/science.1098632).

26. **He, J., S. Choe, R. Walker, P. Di Marzio, D. O. Morgan, and N. R. Landau.** 1995. Human immunodeficiency virus type 1 viral protein R (Vpr) arrests cells in the G_2 phase of the cell cycle by inhibiting p34cdc2 activity. J. Virol. **69:**6705–6711.
27. **Lubkowski, J., F. Yang, J. Alexandratos, A. Wlodawer, H. Zhao, T. R. Burke, Jr., N. Neamati, Y. Pommier, G. Merkel, and A. M. Skalka.** 1998. Structure of the catalytic domain of avian sarcoma virus integrase with a bound HIV-1 integrase-targeted inhibitor. Proc. Natl. Acad. Sci. USA **95:**4831–4836.
28. **Maignan, S., J. P. Guilloteau, Q. Zhou-Liu, C. Clement-Mella, and V. Mikol.** 1998. Crystal structures of the catalytic domain of HIV-1 integrase free and complexed with its metal cofactor: high level of similarity of the active site with other viral integrases. J. Mol. Biol. **282:**359–368.
29. **Mao, P. C., J. F. Mouscadet, H. Leh, C. Auclair, and L. Y. Hsu.** 2002. Chemical modification of coumarin dimer and HIV-1 integrase inhibitory activity. Chem. Pharm. Bull. (Tokyo) **50:**1634–1637.
30. **Morner, A., A. Bjorndal, J. Albert, V. N. Kewalramani, D. R. Littman, R. Inoue, R. Thorstensson, E. M. Fenyo, and E. Bjorling.** 1999. Primary human immunodeficiency virus type 2 (HIV-2) isolates, like HIV-1 isolates, frequently use CCR5 but show promiscuity in coreceptor usage. J. Virol. **73:** 2343–2349.
31. **Naumann, T. A., and W. S. Reznikoff.** 2002. Tn5 transposase active site mutants. J. Biol. Chem. **277:**17623–17629.
32. **Naumann, T. A., and W. S. Reznikoff.** 2000. Trans catalysis in Tn5 transposition. Proc. Natl. Acad. Sci. USA **97:**8944–8949.
33. **Nissley, D. V., P. L. Boyer, D. J. Garfinkel, S. H. Hughes, and J. N. Strathern.** 1998. Hybrid Ty1/HIV-1 elements used to detect inhibitors and monitor the activity of HIV-1 reverse transcriptase. Proc. Natl. Acad. Sci. USA **95:**13905–13910.
34. **Pluymers, W., E. De Clercq, and Z. Debyser.** 2001. HIV-1 integration as a target for antiretroviral therapy: a review. Curr. Drug Targets Infect. Disord. **1:**133–149.
35. **Pluymers, W., N. Neamati, C. Pannecouque, V. Fikkert, C. Marchand, T. R. Burke, Jr., Y. Pommier, D. Schols, E. De Clercq, Z. Debyser, and M. Witvrouw.** 2000. Viral entry as the primary target for the anti-HIV activity of chicoric acid and its tetra-acetyl esters. Mol. Pharmacol. **58:**641–648.
36. **Rice, P. A., and T. A. Baker.** 2001. Comparative architecture of transposase and integrase complexes. Nat. Struct. Biol. **8:**302–307.
37. **Sarnovsky, R. J., E. W. May, and N. L. Craig.** 1996. The Tn7 transposase is a heteromeric complex in which DNA breakage and joining activities are distributed between different gene products. EMBO J. **15:**6348–6361.
38. **Taganov, K. D., I. Cuesta, R. Daniel, L. A. Cirillo, R. A. Katz, K. S. Zaret, and A. M. Skalka.** 2004. Integrase-specific enhancement and suppression of retroviral DNA integration by compacted chromatin structure in vitro. J. Virol. **78:**5848–5855.
39. **van Gent, D. C., K. Mizuuchi, and M. Gellert.** 1996. Similarities between initiation of V(D)J recombination and retroviral integration. Science **271:** 1592–1594.
40. **Wang, J. Y., H. Ling, W. Yang, and R. Craigie.** 2001. Structure of a two-domain fragment of HIV-1 integrase: implications for domain organization in the intact protein. EMBO J. **20:**7333–7343.
41. **Williams, T. L., E. L. Jackson, A. Carritte, and T. A. Baker.** 1999. Organization and dynamics of the Mu transpososome: recombination by communication between two active sites. Genes Dev. **13:**2725–2737.
42. **Yang, Z. N., T. C. Mueser, F. D. Bushman, and C. C. Hyde.** 2000. Crystal structure of an active two-domain derivative of Rous sarcoma virus integrase. J. Mol. Biol. **296:**535–548.
43. **Zhao, H., N. Neamati, H. Hong, A. Mazumder, S. Wang, S. Sunder, G. W. Milne, Y. Pommier, and T. R. Burke, Jr.** 1997. Coumarin-based inhibitors of HIV integrase. J. Med. Chem. **40:**242–249.